Near-Nadir Microwave Specular Returns from the Sea Surface—Altimeter Algorithms for Wind and Wind Stress

JIN WU

Air–Sea Interaction Laboratory, Graduate College of Marine Studies, University of Delaware, Lewes, Delaware

(Manuscript received 24 June 1991, in final form 10 December 1991)

ABSTRACT

Two approaches have been adopted to construct altimeter wind algorithms: one is based on the mean-square sea surface slope, and the other is based on the Seasat scatterometer wind. Both types of algorithms are critically reviewed with respect to the mechanism governing near-nadir radar sea returns and the comparison between altimeter and buoy winds. A new algorithm is proposed; it is deduced on the basis of microwave specular reflection and is finely tuned with buoy-measured winds. On the basis of this algorithm and the formula of the wind-stress coefficient, a simple wind-stress algorithm is also proposed.

1. Introduction

The remote sensing of sea surface winds with an altimeter is based on specular returns from ocean ripples. The most comprehensive data on fine sea surface structures reported by Cox and Munk (1954) were analyzed earlier to deduce quantitative variations of the mean-square slope with wind velocity, as well as its spectral compositions (Wu 1972). At low winds ($U_{10} < 7$ m s^{-1}), the shortest waves contributing to fine structures are in the gravity region ($\lambda > 1.73$ cm), where U_{10} is the wind velocity at 10 m above the mean sea surface and λ is the length of the ocean waves. Capillary waves start to contribute to the mean-square slope at higher wind velocities; the length of the shortest capillary waves making such contributions decreases as the wind velocity increases. Portions of these results were used by Brown (1979) to construct the so-called analytical algorithm for altimeter winds. Subsequently, empirical algorithms were proposed by Chelton and McCabe (1985) and Chelton and Wentz (1986) on the basis of Seasat scatterometer winds. Finally, these algorithms were compared with buoy-measured sea surface winds (Dobson et al. 1987); the analytical algorithm was suggested to provide smaller mean-square errors than the empirical algorithms.

A systematic error, however, is found to be associated with the analytical algorithm; the latter also did not take into account the difference between microwave and optical reflections from the sea surface. In the meantime, the Seasat scatterometer wind was questioned recently by Woiceshyn et al. (1986); this is further complicated by the fact that no analytical basis was provided for the empirical algorithm. A new altimeter wind algorithm is proposed; it is tied in closely with the physical principle and finely adjusted with buoy winds. A recent World Ocean Circulation Experiment–National Aeronautics and Space Administration (WOCE–NASA) workshop called for a continued research on the microwave backscatter at low incidence angles from the sea surface, leading to a refined altimeter wind-speed algorithm (Chelton 1988); the present effort is an attempt in that direction.

2. Previous studies on ocean ripples and altimeter algorithms

a. *Structures of sea surface ripples*

Cox and Munk (1954) determined slopes of ocean ripples from the brightness distribution in photographs of sun glitters on the sea surface. Directional mean-square slopes were obtained from these distributions.

The mean-square slope of sea surface $\overline{s^2}$ can be related to the directional wavenumber spectrum $\psi(\mathbf{k})$ as (Phillips 1977)

$$\overline{s^2} = \int_{k_0}^{k_\nu} k^2 \psi(\mathbf{k}) d\mathbf{k}$$

$$\psi(\mathbf{k}) = (B/\pi) k^{-4} \quad k_\gamma > k > k_0$$

$$\psi(\mathbf{k}) = (B'/\pi) k^{-4} \quad k_\nu > k > k_\gamma, \qquad (1)$$

where $\mathbf{k}$ and k are, respectively, the wavenumber vector and scalar; k_0 is at the spectral maximum; gravity and surface tension have the same quantitative effect on the wave propagation at k_γ; k_ν is the neutrally stable wavenumber; and B and B' are spectral coefficients

Corresponding author address: Dr. Jin Wu, University of Delaware, Air–Sea Interaction Laboratory, College of Marine Sciences, Lewes, DE 19958.

for the gravity and capillary ranges, respectively. Although the spectrum in the equilibrium range near the spectral peak was found to follow $k^{-3.5}$ (Phillips 1985), the k^{-4} form shown above still holds at high wavenumbers (Banner et al. 1989) and is consistent with radar sea returns (Wu 1990b). The spectral coefficients B and B' were determined from the results of Cox and Munk to have values of 4.6×10^{-3} and 3.15×10^{-2}, respectively (Wu 1972, 1990a).

According to Eq. (1), only ocean waves on the high-wavenumber side of the spectral peak contribute to the mean-square slope. The wavenumber at the spectral peak can be approximated by $k_0 = g/U_{10}^2$, in which g is the gravitational acceleration. At low winds ($U_{10} < 7$ m s^{-1}), the shortest contributing component was found to be at the wavenumber of about 2.5 rad cm^{-1}; it is in the gravity range, as the wavenumber k_γ dividing the gravity and capillary regions is at about 3.6 rad cm^{-1}. The upper cutoff wavenumber k_h at high winds can be found from

$$\overline{s^2} = B \ln(k_\gamma U_{10}^2/g) + B' \ln(k_h/k_\gamma). \quad (2)$$

The variation of mean-square slope with the wind velocity, therefore, follows a two-segment trend; only the first term on the right-hand side of Eq. (2) contributes at low winds, and both terms contribute at high winds. The mean-square slope increases much more rapidly with the wind velocity at high winds, where capillary waves are involved; this can also be seen from Eq. (2), with the coefficient B' having a much greater value than B.

Quantitatively, Cox and Munk's (1954) data were verified to follow (Wu 1972, 1990a)

$$\overline{s^2} = (0.90 + 1.20 \ln U_{10}) \times 10^{-2}, \quad U_{10} < 7 \text{ m s}^{-1} \quad (3)$$

$$\overline{s^2} = (-8.40 + 6.00 \ln U_{10}) \times 10^{-2}, \quad U_{10} > 7 \text{ m s}^{-1}, \quad (4)$$

where U_{10} is in meters per second. Again, the first expression represents the contribution from the gravity range, down to the wavelength of about 2.5 cm; and the second includes the additional contribution from this wavelength to the capillary range. The ratio between the crosswind and upwind–downwind mean-square slopes was found to be almost invariant with the wind velocity, having a value of about 0.8.

b. *Development of spaceborne-altimeter algorithms*

1) ANALYTICAL APPROACH

The reflectivity of the sea surface is high over the microwave frequencies at which the satellite altimeter operates (Maul 1985). As the sea surface is roughened by the wind, the incident radiation reflected back to the altimeter decreases. The signal received is expressed as the normalized radar cross section, which is proportional to the ratio between received and transmitted radar powers. The radiation backscattered from the sea surface, of course, depends on its incidence angle. At small incidences for the satellite altimetry, the backscattering is primarily specular reflections (Valenzuela 1978).

The specular-point models were reviewed by Barrick (1974) to offer the following expression for the normalized radar cross section σ_0:

$$\sigma_0 = \pi \sec^4\theta p_s(-\tan\theta, 0^\circ) |R(0^\circ)|^2, \quad (5)$$

where θ is the angle of incidence from the vertical, $R(0^\circ)$ is the Fresnel reflection coefficient of the sea surface at the normal incidence, and p_s is the joint probability density function of surface slopes in the upwind–downwind and crosswind directions. This expression was rewritten by Brown (1979) as

$$\sigma_0 = (\alpha/\overline{s^2}) |R(0^\circ)|^2 \exp(\tan^2\theta/\overline{s^2}), \quad (6)$$

where α is a proportionality constant, depending on the form of the probability density function of slopes; it has a value of unity for the Gaussian form and of 3 for Laplacian or double-sided exponentials. For a nadir-looking altimeter, the above was reduced to

$$\sigma_0(0^\circ) = \alpha |R(0^\circ)|^2/\overline{s^2}. \quad (7)$$

The basic concept of a two-branch variation of the mean-square slope with wind velocity, discussed earlier, was adopted by Brown (1979) to propose the wind algorithm for the *GEOS-3* (13.9-GHz) altimeter;

$$\sigma_0(0^\circ) = -10 \log(0.02098 \ln U_{10} + 0.01075) - 2.1 \quad U_{10} < 9.2 \text{ m s}^{-1}$$

$$\sigma_0(0^\circ) = -10 \log(0.08289 \ln U_{10} - 0.12664) - 2.1 \quad U_{10} > 9.2 \text{ m s}^{-1}, \quad (8)$$

where $\sigma_0(0^\circ)$ is expressed in decibels, and $|R(0^\circ)|^2 = -2.1$ dB. Note that through the matching between the microwave cross section and ship-reported wind, the two curves now intersect at 9.2 m s^{-1}; and that the value of α used appears to be quite smaller than 1, being about 0.7. The above expressions are diagramed in Fig. 1.

Subsequently, the above algorithm was updated by Brown et al. (1981); the update, although slight in the magnitude of radar cross sections, provided even more branches. Later, this multiply branched algorithm was smoothed by Goldhirsh and Dobson (1985) with a fifth-degree polynomial. For the clarity of presentation, both the algorithms of Brown et al. (1981) and Goldhirsh and Dobson (1985), differing insignificantly from Brown's (1979), are not shown in Fig. 1.

2) EMPIRICAL APPROACH

At intermediate incidences (20°–70°), radar returns from the sea surface have been considered to follow the Bragg scattering (Moore 1985); the radar cross sec-

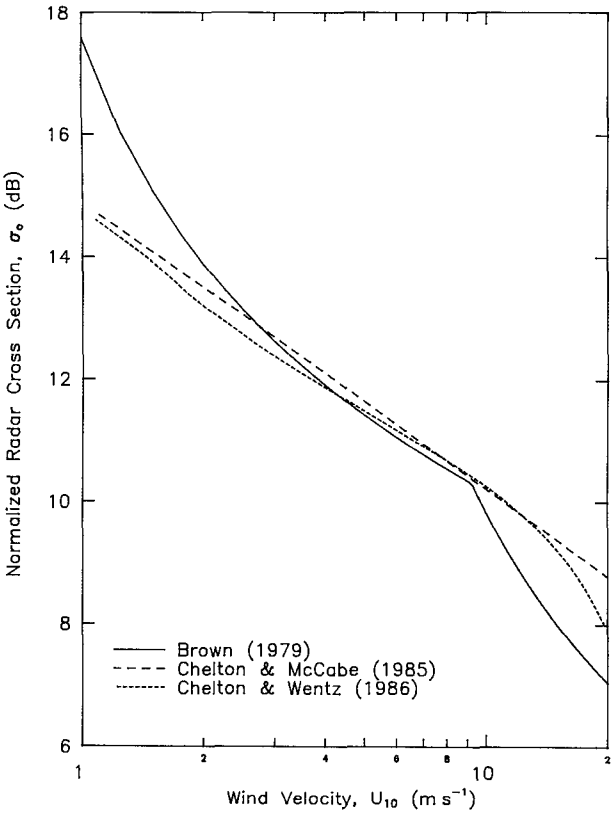

FIG. 1. Normalized radar cross sections predicted by various algorithms.

tion is related to the wind speed in the form of a power law. Adopting this practice, Chelton and McCabe (1985) proposed a similar algorithm for altimeter winds by comparing radar returns from the 13.5-GHz altimeter with those from the 14.6-GHz Seasat scatterometer;

$$\sigma_0 = 10(1.502 - 0.468 \log U_{19.5}), \quad (9)$$

where $U_{19.5}$ (m s^{-1}) is the wind velocity measured at 19.5 m above the mean sea surface. In this derivation, the Seasat data used were those analyzed by Boggs (1981) and Schroeder et al. (1982). Chelton and McCabe (1985) also emphasized the need of a simple model function to avoid double branches contained in the Brown (1979) algorithm and multiple branches in that of Brown et al. (1981). The above expression was modified subsequently by Chelton and Wentz (1986); they used Seasat scatterometer winds calculated from the model function proposed by Wentz et al. (1986). The latter was suggested to contain no systematical errors. Following the same procedure as in Chelton and McCabe (1985), but with this new reference wind, another model was proposed by Chelton and Wentz (1986) in a tabulated form.

Both empirical algorithms discussed above were expressed in terms of the wind speed at the 19.5-m elevation, while that at the 10-m elevation is generally used in the oceanographical community. Consequently, the logarithmic velocity profile is adopted to convert the wind velocity from $U_{19.5}$ to U_{10} (Wu 1968);

$$\frac{(U_{19.5} - U_{10})}{u_*} = \left(\frac{1}{\kappa}\right) \ln(1.95), \quad u_* = C_{10}^{1/2} U_{10}, \quad (10)$$

where u_* is the friction velocity, $\kappa = 0.4$ is the von Kármán constant, and C_{10} is the wind-stress coefficient. The atmospheric surface layer is aerodynamically smooth under very light winds and enters the transition region and becomes aerodynamically rough as the wind velocity increases. The wind-stress coefficients for two cases were proposed by Wu (1980, 1988) to follow

$$C_{10} = [(1/\kappa) \ln(C_{10}^{1/2} U_{10} Z/\nu) + 5.5]^{-2}, \quad U_{10} < 2.4 \text{ m s}^{-1}$$

$$C_{10} = (0.8 + 0.065 U_{10}) \times 10^{-3} \quad U_{10} > 2.4 \text{ m s}^{-1}, \quad (11)$$

where $Z = 10$ m is the standard anemometer height, ν is the kinematic viscosity of air, and U_{10} in the second expression is in meters per second. The algorithms proposed by Chelton and McCabe (1985) and by Chelton and Wentz (1986) were then transferred in terms of U_{10} and are diagramed in Fig. 1.

3. Development of a new algorithm

a. Comments on current algorithms

1) QUANTITATIVE ASPECTS

Although the algorithm of Chelton and Wentz (1986) is also based on the scatterometer winds, it differs from that of Chelton and McCabe (1985) in a couple of essential points. The preference of a simple-varying function was emphasized by Chelton and McCabe, but the algorithm of Chelton and Wentz consists of a rather complex curve having multiple reflection points. The high-wind portion of Chelton and McCabe's was revised downward by Chelton and Wentz. All three algorithms—Brown (1979), Chelton and McCabe (1985), and Chelton and Wentz (1986)—are in better agreements at intermediate winds. At low and high winds, the Brown algorithm deviates obviously from the latter ones; the difference becomes greater as the wind speed decreases at low winds and as the wind speed increases at high winds.

The wind speeds measured from buoys moored in the North Pacific, the North Atlantic, and the Gulf of Mexico during the Geosat mission were compiled by Dobson et al. (1987). The Geosat data within 50 km of buoy locations were processed according to four al-

gorithms proposed by Brown et al. (1981), Goldhirsh and Dobson (1985), Chelton and McCabe (1985), and Chelton and Wentz (1986); they were presented in Figs. 1–4 of Dobson et al. Their comparison of these algorithms are adopted here, as Brown et al.'s algorithm (1981) was discussed earlier to differ insignificantly from Brown's (1979). Furthermore, only three of the four figures are reproduced in Figs. 2a–c, as the data associated with Goldhirsh and Dobson's algorithm are quite similar to those with Brown et al.'s. In order to have a clearer presentation with a somewhat enlarged scale, two data points in Fig. 2a, three in Fig. 2b, and one in Fig. 2c lying outside the frame, are omitted. Nonetheless, the total 121 data points presented in Dobson et al. are used for discussions throughout this article. The root-mean-square errors of altimeter winds deviating from the corresponding buoy winds from all the data points were calculated by Dobson et al.; their results are compiled in Table 1. As pointed out by Dobson et al., the Brown et al. algorithm (either original or smoothed) is seen in Table 1 to provide smaller root-mean-square errors than two empirical algorithms.

The data of buoy winds compiled by Dobson et al. (1987) provide the most valuable sea-surface truth for constructing the altimeter wind algorithm. An attempt is thus made to examine more rigorously the comparisons between the altimeter and buoy winds, especially there appears to be some definite trends shown in Figs. 2a–c. Differentials between the Geosat wind determined with each one of the four algorithms and the corresponding buoy wind are obtained. The differential is the Geosat wind deviating from the diagonal line shown in the figure and represented by one of the following expressions:

$$U_{ab} = U_b,\ U_{ag} = U_b,\ U_{am} = U_b \quad \text{and} \quad U_{aw} = U_b, \tag{12}$$

where U_b is the buoy wind speed; and U_{ab}, U_{ag}, U_{am}, and U_{aw} are, respectively, the altimeter wind speeds determined from the algorithms of Brown et al. (1981), Goldhirsh and Dobson (1985), Chelton and McCabe (1985), and Chelton and Wentz (1986). The results are shown in the left-hand column of Fig. 3. A system-

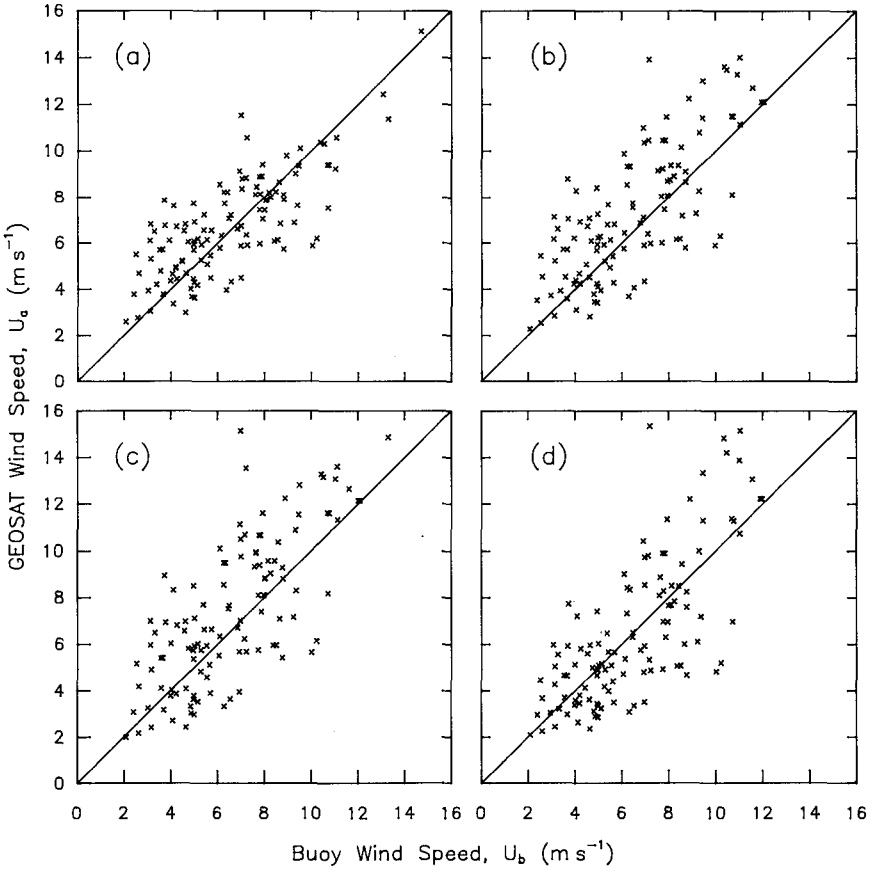

FIG. 2. Comparisons between Geosat altimeter winds deduced from various algorithms and buoy winds. The altimeter winds were from (a) Brown et al. (1981), (b) Chelton and McCabe (1985), (c) Chelton and Wentz (1986), and (d) the present algorithm; (a), (b), and (c) are reproduced from Dobson et al. (1987).

TABLE 1. Root-mean-square errors between altimeter and buoy winds reported by Dobson et al. (1987).

	Brown et al. (1981)	Goldhirsh and Dobson (1985)	Chelton and McCabe (1985)	Chelton and Wentz (1986)
Root-mean-square error (m s^{-1})	1.70	1.82	2.37	2.31

atic error is clearly displayed for two analytical algorithms; they overpredict the wind speed at low winds and underpredict at high winds. A similar behavior was also detected for the Seasat scatterometer (Woiceshyn et al. 1986). Consequently, when the scatterometer winds were used to deduce the altimeter algorithm as in Chelton and McCabe and in Chelton and Wentz, such a systematic discrepancy was much reduced. There is no doubt, however, that the root-mean-square errors are greater for two empirical algorithms, as indicated by Dobson et al. (1987).

In order to rectify the systematic error discussed above, straight lines are fitted to the wind-speed deviations shown in the left-hand column of Fig. 3; subsequently, the fitted lines are combined with Eq. (12) to obtain

$$U_{ab} = 3.88 + 0.453U_b$$
$$U_{ag} = 4.79 + 0.358U_b$$
$$U_{am} = 2.09 + 0.832U_b$$
$$U_{aw} = 2.11 + 0.805U_b. \quad (13)$$

Deviations of the Geosat wind from one of the above expressions are again found and presented in the right-hand column of Fig. 3; they are now seen to distribute rather evenly around $\Delta U = 0$ m s^{-1}.

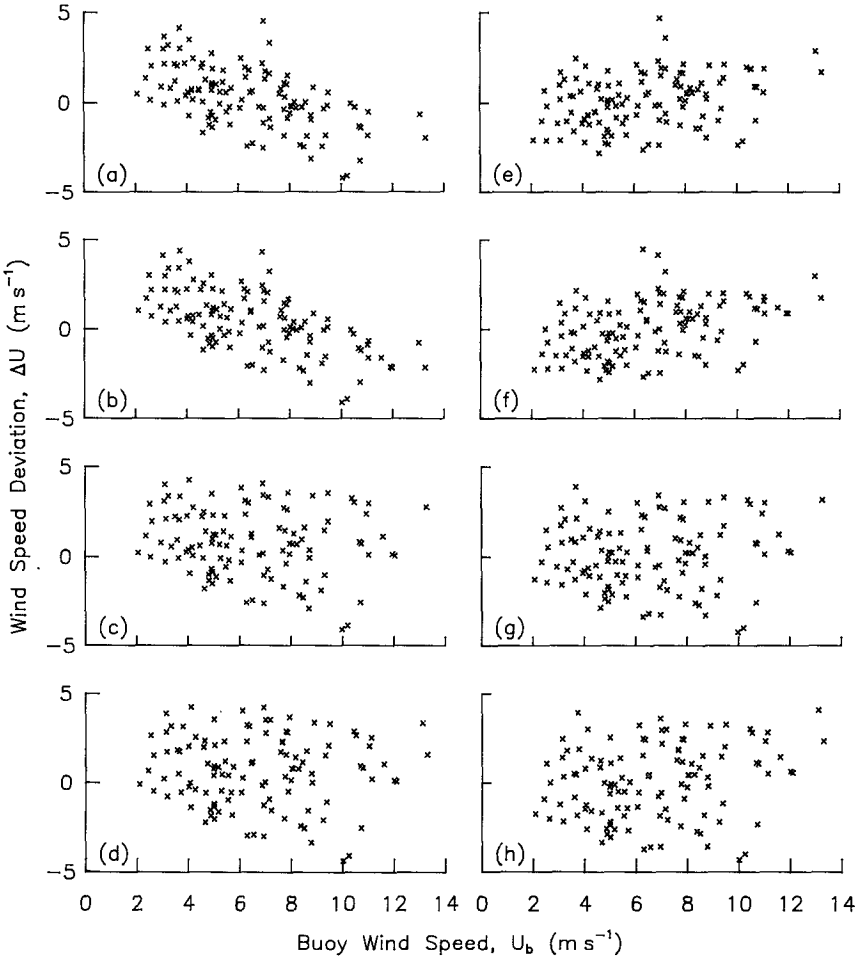

FIG. 3. Wind-speed deviations from proposed algorithms and from refitted lines. The deviations in the left-hand column are obtained with Eq. (12) and those in the right-hand column with Eq. (13). The algorithms used are Brown (1981) (a) and (e), Goldhirsh and Dobson (1985) (b) and (f), Chelton and McCabe (1985) (c) and (g), and Chelton and Wentz (1986) (d) and (h).

In summary, while the root-mean-square error is always important in comparing algorithms, the systematic deviation is even more critical in judging the physical soundness of the algorithm. The data are seen in Fig. 3 to follow Eq. (13) much more closely than the original algorithms represented by Eq. (12). Although offering a smaller mean-square error, the wind speed deduced from algorithms of Brown et al. (1981) and Goldhirsh and Dobson (1985) deviates systematically from the buoy wind. Ideally, the intercept between the predicted and measured winds should be zero, and the coefficient should have a value of unity. Instead, the intercepts shown in Eq. (13) are significant, and the coefficients are smaller than unity. In both of these aspects, the algorithms of Chelton and McCabe (1985) and of Chelton and Wentz (1986) appear to provide a better overall representation of buoy winds. It is therefore of interest to understand these results: the misrepresentation of overall trend by the analytical algorithm and a closer representation in the trend by the empirical algorithms, which have somewhat greater errors. The latter is believed to be simply that buoy winds undoubtedly contained errors; the former is discussed below.

2) PHYSICAL DEFICIENCY

An analytical algorithm is, of course, preferred, but the spectral resolution of fine sea surface structures was not taken into account. In other words, the total mean-square sea surface slope was used without considering its contributions from various surface wavelength regions. This is important, as specular reflections from the sea surface observed with microwave sensors may differ from those with optical sensors (Brown 1978; Kwoh et al. 1988). A minor point is that the value of proportionality constant α also appears to be improperly small. In the meantime, the empirical approach needs physical justifications since the formulas were constructed on the basis of the Seasat scatterometer wind. The latter cannot be viewed as the ground truth, especially when the scatterometer algorithm has been seriously challenged (Woiceshyn et al. 1986). The current scatterometer algorithm was further questioned by Wu (1990b); the exponent of power law, which is the core of the algorithm, was shown to vary systematically with the radar wavelength and incidence angle instead of having a nearly constant value. It may therefore be advisable to follow the analytical approach.

b. Proposal of new algorithms

1) WIND-SPEED ALGORITHM

As discussed earlier, the altimeter returns consist of specular reflections from small facets distributed over the illuminated area. Only those facets having their radius of curvature larger than the microwave length can contribute to the altimeter returns (Ulaby et al. 1986; Kwoh et al. 1988). Very little is known about the surface curvature of facets; the above condition, however, can be approximately satisfied by considering that surface waves shorter than the radar wavelength should not contribute to specular returns (Brown 1978). The X-band radar was used for the Geosat altimeter; it has a wavelength of about 2.16 cm, differing only very slightly from the cutoff wavelength of about 2.5 cm for the mean-square slope shown in Eq. (3). Consequently, this formula should be used not only for low winds, but also for high winds with its extension.

The distribution of ripple slopes is nearly Gaussian (Cox and Munk 1954); the proportionality constant α should have a value very close to unity. A new algorithm is then obtained by substituting Eq. (3) into Eq. (7) with $\alpha = 1$; it is shown as a solid curve in Fig. 4a. In the figure, three currently used algorithms are also reproduced from Fig. 1. The new algorithm first of all is continuous with no branches; it is also seen to suppress the curving up of Brown's (1979) algorithm at low winds and the curving down at high winds. These curving trends are the main cause of systematical errors displayed in Figs. 3a,b. In the meantime, the new algorithm is seen for wind speeds of about 2 m s^{-1} and greater to be almost parallel with algorithms of Chelton and McCabe (1985) and Chelton and Wentz (1986), which as discussed earlier follow well the overall trend of buoy winds. Since the altimeter was not fully calibrated, the trend is actually of a greater interest than the absolute return. Such a parallel trend indicates on one hand that the present analytical results may provide the justification of empirical algorithms and on the other that the present analytical algorithm is supported by buoy winds.

For the best matching between the new and the empirical algorithms, the spacing between them is seen in Fig. 4a to be about 1.9 dB, depending on the value of α discussed earlier. This is also reasonable; since the power across the radar footprint does not fall sharply to zero at the half-power point, the theoretical prediction with the half-power beamwidth is generally about 1–2 dB too high (Wetzel 1990). The new algorithm can be justifiably tuned with buoy winds, to have a downward parallel shift of 1.9 dB; see Fig. 4b. The new algorithm can now be written as

$$\sigma_0 = -4 - 10 \log \overline{s_g^2}$$
$$= -4 - 10 \log(0.009 + 0.012 \ln U_{10}), \quad (14)$$

in which again σ_0 is in decibels, and $\overline{s_g^2}$ is designated as the mean-square slope shown in Eq. (3) for all wind speeds. Referring to Fig. 4b, the main difference between the current algorithm and those proposed earlier is essentially at high winds with wind speeds beyond 10 m s^{-1}. Here the current algorithm is believed to be

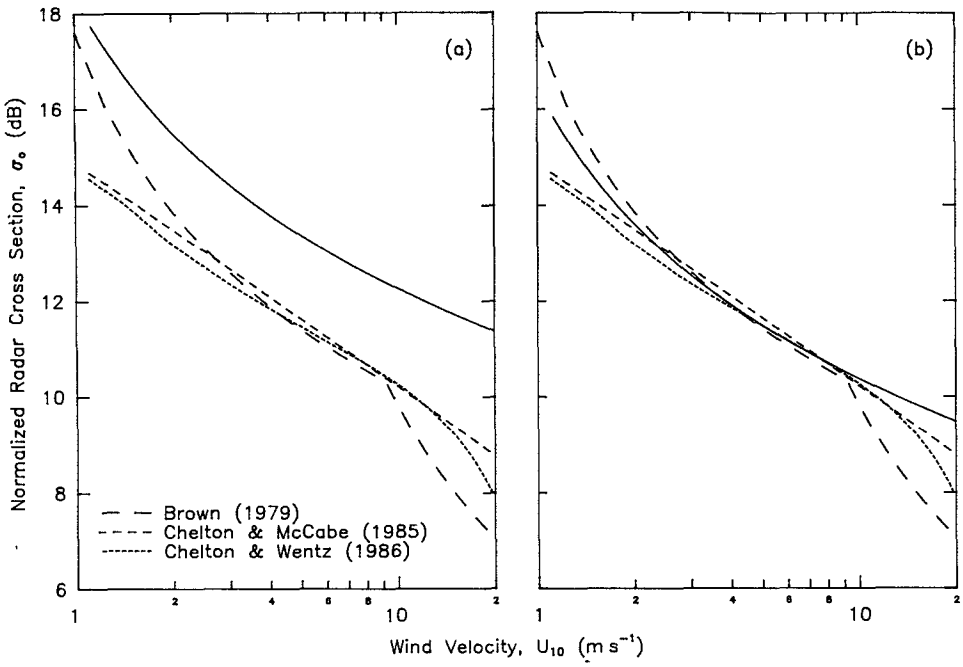

FIG. 4. A new algorithm for altimeter winds and comparisons between this and previously proposed algorithms. The new algorithm is shown as a solid curve in (a) and is adjusted with buoy winds in (b).

preferable by taking into account the spectral composition of mean-square slopes. Short gravity waves and gravity-capillary waves are believed to be saturated at relatively low winds, at least below 10 m s^{-1} (Banner et al. 1989; Wu 1990b). The increase of mean-square slope at high winds was shown earlier to come mainly from the capillary region (Wu 1990a); these short waves cannot produce altimeter returns.

Values of (σ_0, U_b) can be obtained from Figs. 2a–c; actually, only one of the figures is sufficient, while the others are used to verify these values. Having this set of data, the downward tuning discussed above was also determined by fitting the proposed analytical algorithm repeatedly to the data; the best fit was found to be provided by the downward shifting of about 2.1 dB. This differs little from the value of 1.9 dB used in Eq. (14).

With the values of (σ_0, U_b), the altimeter winds can be obtained from Eq. (14) and presented in Fig. 2d. The present algorithm is seen to avoid the systematic error shown in Fig. 2a and to reduce the scatterings shown in Figs. 2b,c. The latter is particularly important, as the analytical algorithm proposed by Brown (1979) is upgraded here to limit quantitative comparisons to those between the present and the empirical algorithms. The root-mean-square error of the present algorithm is calculated from all the data points to be 1.92 m s^{-1}, which is smaller than the values of two empirical algorithms shown in Table 1. As discussed earlier, the algorithm of Brown et al. (1981) is an upgraded version of Brown's (1979). Recently, the empirical algorithm of Chelton and Wentz (1986) was also modified by Witter and Chelton (1991) by correcting a calibration difference between Seasat and Geosat altimeters. The root-mean-square error of this modified algorithm is smaller, being very close to the value cited above, but the difference between the original and modified algorithms is primarily at high winds. Consequently, the tuning discussed here is largely unaffected. In any event, further studies are needed to see whether the difference in errors contained in the previous and present algorithms is statistically significant.

2) WIND-STRESS ALGORITHM

Oceanographical phenomenon are generally governed by the wind stress rather than the wind speed. In fact, much effort in developing the scatterometer algorithm has been presently directed toward the determination of wind stress (Wu 1989). Along the same line, an altimeter algorithm for the wind-friction velocity is deduced in the following.

Using the formulas shown in Eq. (11), the wind-speed algorithm shown in Eq. (14) is diagramed in Fig. 5 in terms of the friction velocity. The smooth curve can be represented very closely by

$$\sigma_0 = -7.6 \log(\ln u_* + 3.85) + 13.85, \quad (15)$$

where u_* is expressed in meters per second.

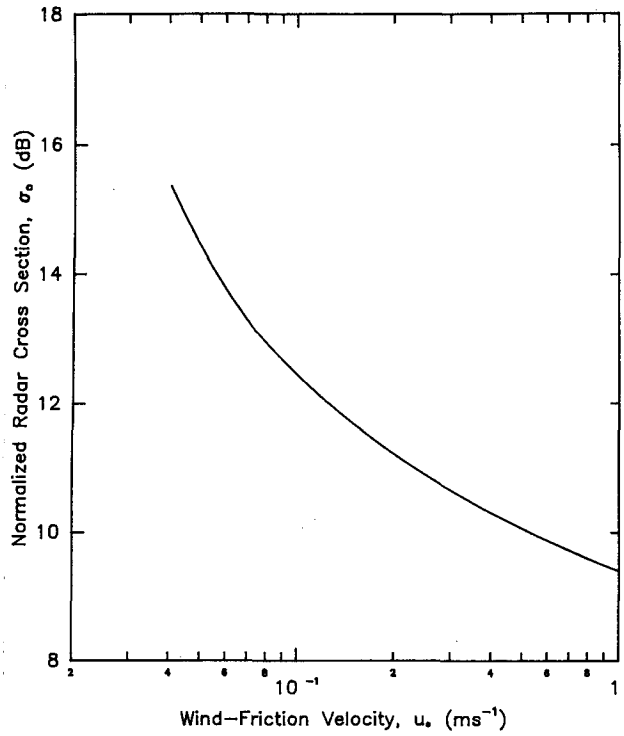

FIG. 5. Variation of altimeter returns with the friction velocity—a wind-stress algorithm.

4. Concluding remarks

The altimeter wind algorithms have been developed along two lines. The analytical algorithm was deduced from the optical reflections, which differ from the microwave returns; the empirical algorithms were deduced from the scatterometer winds, which cannot serve as the ground truth. The present algorithm conforms closely with the governing physical principle; only surface wave components longer than the radar wavelength are included. The systematical errors contained in the previous analytical algorithm is avoided by correcting its physical deficiency, while the similarity between the proposed and empirical algorithms provides the justification for the latter. In addition, the mean-square error of the present proposal is also smaller than those of the empirical algorithms. It should be emphasized, however, that a true validation should be based on the altimeter returns at various wind speeds; the latter appears to be the most pressing study. The current situation becomes further complicated at high winds, at which the scatterometer data used for establishing the empirical algorithms and for tuning the present proposal also becomes unavailable. The algorithm construction is indeed a continuing process; this is particularly true for the satellite altimetry that has been suggested to be unique among spaceborne oceanographic remote-sensing techniques in its long history of development and steady improvement of accuracy (Chelton 1988).

Acknowledgments. The author is very grateful for sponsorships of his work provided by the Remote Sensing Program (N00014-89-J-3226), Office of Naval Research, the Ocean Dynamics Program (NAGW-2981), National Aeronautics and Space Administration, and the Physical Oceanography Program (OCE-8716519), National Science Foundation.

REFERENCES

Banner, M. L., I. S. F. Jones, and J. C. Trinder, 1989: Wavenumber spectra of short gravity waves. *J. Fluid Mech.*, **198,** 321–344.

Barrick, D. E., 1974: Wind dependence of quasi-specular microwave sea scatter. *IEEE Trans. Anten. Propag.*, **AP-22,** 135–136.

Boggs, D. H., 1981: The Seasat scatterometer model function: The genesis of SASS-1. Rep. 622-630, Jet Propulsion Lab., Pasadena, CA.

Brown, G. S., 1978: Backscattering from a Gaussian distributed, perfectly conducting, rough surface. *IEEE Trans. Anten. Propag.*, **AP-26,** 472–482.

——, 1979: Estimation of surface wind speeds using satellite-borne radar measurements at normal incidence. *J. Geophys. Res.*, **84,** 3974–3978.

——, G. S., H. R. Stanley, and N. A. Roy, 1981: The wind-speed measurement capability of spaceborne radar altimeters. IEEE *J. Oceanic Eng.*, **OE-6,** 59–63.

Chelton, D. B., 1988: WOCE/NASA altimeter algorithm workshop. U.S. WOCE Tech. Rep. 2, U.S. Planning Office for WOCE, College Station, TX.

——, and P. J. McCabe, 1985: A review of satellite altimeter measurement of sea surface wind speed: With a proposed new algorithm. *J. Geophys. Res.*, **90,** 4707–4720.

——, and F. J. Wentz, 1986: Further development of an improved altimeter wind speed algorithm. *J. Geophys. Res.*, **91,** 14 250–14 260.

Cox, C. S., and W. H. Munk, 1954: Measurement of the roughness of the sea surface from photographs of the sun's glitter. *J. Opt. Soc. Amer.*, **44,** 838–850.

Dobson, E., F. Monaldo, J. Goldhirsh, and J. Wilkerson, 1987: Validation of Geosat altimeter-derived wind speeds and significant wave heights using buoy data. *J. Geophys. Res.*, **92,** 10 719–10 731.

Goldhirsh, J., and E. B. Dobson, 1985: A recommended algorithm for the determination of ocean surface wind speed using a satellite-borne radar altimeter. JHU/APL Tech. Rep. SIR85U-005, Applied Physics Lab., Johns Hopkins Univ., Laurel, MD.

Kwoh, D. S. W., B. M. Lake, and H. Rungaldier, 1988: Microwave scattering from internal wave modulated surface waves: A shipboard real aperture coherent radar study in the Georgia Strait Experiment. *J. Geophys. Res.*, **93,** 12 235–12 248.

Maul, G. A., 1985: *Introduction to Satellite Oceanography.* Martinus Nijhoff Publishers.

Moore, R. K., 1985: Radar sensing of the ocean. *IEEE J. Oceanic Eng.*, **OE-10,** 84–112.

Phillips, O. M., 1977: *The Dynamics of the Upper Ocean.* Cambridge University Press.

——, 1985: Spectral statistical properties of the equilibrium range in the wind-generated gravity waves. *J. Fluid Mech.*, **156,** 506–531.

Schroeder, L. C., D. H. Boggs, G. Dome, I. M. Halberstam, W. L. Jones, W. J. Pierson, and F. J. Wentz, 1982: The relationship between wind vector and normalized radar cross section used to derive *Seasat-A* satellite scatterometer winds. *J. Geophys. Res.*, **87,** 3318–3336.

Ulaby, F. T., R. K. Moore, and A. K. Fung, 1986: *Microwave Remote Sensing—Active and Passive.* Artech House.

Valenzuela, G. R., 1978: Theories for the interaction of electromagnetic and oceanic waves—A review. *Bound.-Layer Meteor.*, **13,** 61–85.

Wentz, F. J., L. A. Mattox, and S. Peteherych, 1986: New algorithms for microwave measurements of ocean winds: Applications to Seasat and SSM/I. *J. Geophys. Res.*, **91,** 2289–2307.

Wetzel, L. B., 1990: Sea clutter. Rep. 9244, Naval Research Lab., Washington, D.C.

Witter, D. L., and D. B. Chelton, 1991: A Geosat altimeter wind speed algorithm and a method for altimeter wind speed algorithm development. *J. Geophys. Res.*, **96,** 8853–8860.

Woiceshyn, P. M., M. G. Wurtele, D. H. Boggs, L. F. McGoldrick, and S. Peteherych, 1986: The necessity for a new parameterization of an empirical model for wind/ocean scatterometry. *J. Geophys. Res.*, **91,** 2273–2288.

Wu, J., 1968: Laboratory studies of wind–wave interactions. *J. Fluid Mech.*, **34,** 91–111.

——, 1972: Sea surface slope and equilibrium wind-wave spectra. *Phys. Fluids,* **15,** 741–747.

——, 1980: Wind-stress coefficients over sea surface near neutral conditions—A revisit. *J. Phys. Oceanogr.*, **10,** 727–740.

——, 1988: Wind-stress coefficients at light winds. *J. Atmos. Oceanic Technol.*, **5,** 885–888.

——, 1989: Dependence of microwave sea returns on wind-friction velocity under varied atmospheric stability conditions. *IEEE J. Oceanic Eng.*, **OE-14,** 254–258.

——, 1990a: Mean-square slopes of the wind-disturbed water surface—Their magnitude, directionality and composition. *Radio Sci.*, **25,** 37–48.

——, 1990b: Radar sea returns—Ocean-ripple spectrum and breaking-wave influence. *J. Phys. Oceanogr.*, **20,** 1985–1993.